



This is a repository copy of *'Resin welding': a novel route to joining acrylic composite components at room temperature.*

White Rose Research Online URL for this paper:

<https://eprints.whiterose.ac.uk/210421/>

Version: Published Version

Article:

Devine, M. orcid.org/0009-0000-9633-1733, Bajpai, A., Ó Brádaigh, C.M. et al. (1 more author) (2024) 'Resin welding': a novel route to joining acrylic composite components at room temperature. *Composites Part B: Engineering*, 272. 111212. ISSN 1359-8368

<https://doi.org/10.1016/j.compositesb.2024.111212>

Reuse

This article is distributed under the terms of the Creative Commons Attribution (CC BY) licence. This licence allows you to distribute, remix, tweak, and build upon the work, even commercially, as long as you credit the authors for the original work. More information and the full terms of the licence here:

<https://creativecommons.org/licenses/>

Takedown

If you consider content in White Rose Research Online to be in breach of UK law, please notify us by emailing eprints@whiterose.ac.uk including the URL of the record and the reason for the withdrawal request.



eprints@whiterose.ac.uk
<https://eprints.whiterose.ac.uk/>



'Resin welding': A novel route to joining acrylic composite components at room temperature

Machar Devine^a, Ankur Bajpai^a, Conchúr M. Ó Brádaigh^b, Dipa Ray^{a,*}

^a School of Engineering, Institute for Materials and Processes, The University of Edinburgh, Sanderson Building, Robert Stevenson Road, Edinburgh, EH9 3FB, Scotland, United Kingdom

^b Department of Materials Science & Engineering, Faculty of Engineering, University of Sheffield, Sir Robert Hadfield Building, Mappin Street, Sheffield S1 3JD, United Kingdom

ARTICLE INFO

Handling Editor: Prof. Ole Thomsen

Keywords:

Thermoplastic resin
Adhesion
Mechanical testing
Joints/joining
Thermoplastic welding

ABSTRACT

The solubility of acrylic polymer in its own liquid monomer creates the opportunity to 'weld' acrylic-matrix (Elium®) composites without the application of heat. In this method, termed *resin welding*, acrylic monomeric resin is infused between acrylic-matrix composite parts. The resin dissolves and diffuses into the acrylic matrix and creates a continuous material, and a strong bond, when it polymerises, without the sensitivities of traditional welding methods to adherend or bondline thickness. Single lap shear testing was conducted on resin-welded and adhesively-bonded coupons with varying bondline thicknesses and filling fibres, and the bonding and fracture mechanisms were investigated using SEM and the diffusion of dyed acrylic resin. The highest bond strength of resin-welded coupons reached 27.9 MPa, which is 24 % higher than the strongest weld reported in the literature, indicating that resin welding is a promising alternative to traditional bonding and welding methods for acrylic-matrix composites.

1. Introduction

Recyclable acrylic-matrix composites produced using infusible acrylic resins are a possible route towards creating a circular economy in the composites industry. They have been shown to have excellent mechanical properties on par with or even exceeding the properties of non-recyclable, but widely used, epoxy composites [1,2]. These resins are largely composed of methyl methacrylate (MMA) monomers which polymerise in-situ to form a poly-methyl methacrylate (PMMA) based copolymer during composite manufacturing. The resin therefore has a low viscosity, enabling its use in the manufacture of large composite structures such as the 62 m long acrylic-matrix wind turbine blade recently manufactured as part of the ZEBRA project, led by IRT Jules Verne [3].

These large structures are often manufactured in multiple sections which then require joining together. A common method of manufacturing wind turbine blades, for example, is to infuse two shells separately and join them together with a shear web or spar in the centre [4]. The current method of joining these parts is to use adhesives, however the use of thermoplastic matrices such as acrylic provides the opportunity to use welded joints instead. It has been suggested that

higher joint strengths, greater fatigue life and faster processing times could be achieved through welding [5].

There are several types of welding which can be used for thermoplastic polymer matrix composites. Literature on the welding of acrylic-matrix composites has concentrated on fusion welding in which heat is applied to the adherends and the polymer matrix melts and interdiffuses when pressure is applied to the joint. Heat can be applied in several ways: for example, via a heating element in the joint (resistive and inductive welding), through frictional heating (ultrasonic, vibrational or spin welding), or via the direct heating of the adherends (e.g. with infrared or other radiation, a hot-plate, or hot gas) [6].

Four methods of welding acrylic-matrix composites are discussed in the literature: resistance, induction, ultrasonic and infra-red welding [5, 7–10]. Resistance and induction welding in glass fibre reinforced acrylic composites have been explored by Murray et al. using single lap shear testing [5]. In this study, single lap resistance welds had average single lap strengths ranging between 19.1 MPa and 22.4 MPa depending on the heating element used. The fatigue limit, defined by the authors as the stress at which a coupon survived 10 million cycles at a stress ratio *R* of 0.1 and frequency of 10 Hz, was reported to be 5 MPa for resistance welds joined using a carbon fibre heating element [5]. Coupons joined

* Corresponding author.

E-mail address: dipa.roy@ed.ac.uk (D. Ray).

<https://doi.org/10.1016/j.compositesb.2024.111212>

Received 12 October 2023; Received in revised form 18 December 2023; Accepted 8 January 2024

Available online 9 January 2024

1359-8368/© 2024 The Authors. Published by Elsevier Ltd. This is an open access article under the CC BY license (<http://creativecommons.org/licenses/by/4.0/>).

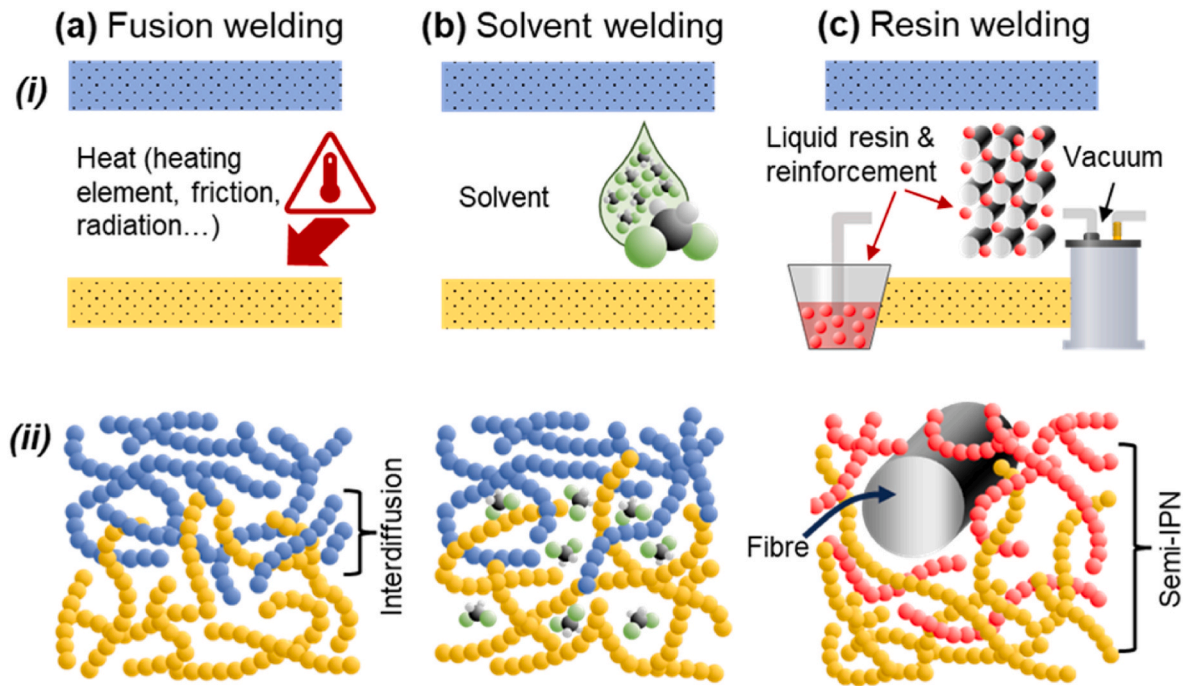


Fig. 1. Illustrations of the welding methods for thermoplastic polymers and composites. (a) Fusion bonding increases polymer mobility by heating. Applying pressure allows the polymer to interdiffuse. (b) Solvent welding increases polymer mobility by dissolution at room temperature, but solvent remains trapped in the polymer. (c) In the resin welding method, the acrylic monomer acts as a reactive solvent and polymerises around the adherend matrix. The same mechanism is applicable to reactive solvent cements.

via induction welding with a carbon fibre heating element reached a lower average single lap shear strength of 20.4 MPa. For comparison, several adhesive joints were also tested, although the highest adhesive single lap strength and fatigue limit—achieved using Plexus MA310 methacrylate adhesive—were only 17.4 MPa and 3 MPa respectively.

In another study, ultrasonic welding of carbon fibre reinforced acrylic has also been studied by Bhudolia et al. [7,9]. Similar results were achieved to Ref. [5], with welded single lap joints reaching a strength of 18.9 MPa with proper optimisation, which was 33 % higher than the strength of adhesive bonds (14.2 MPa) made with Bostik SAF 30-5 methacrylate adhesive. The fatigue strength of ultrasonically welded single lap coupons at 10^5 cycles ($R = 0.1$, frequency = 5 Hz) was also 12 % higher than that of adhesive bonds (7.26 MPa and 6.48 MPa respectively), although this reduced to a 7 % difference at 10^7 cycles.

The fourth welding method demonstrated for acrylic-matrix composites in the literature is infrared welding. Perrin et al. [10] obtained single lap shear strengths of 12.3 MPa using this method, although this was improved up to 19.1 MPa by the addition of a small amount of crosslinker to the acrylic matrix of the adherends.

Although each welding method has its advantages and disadvantages, a common requirement for all three is intimate contact between the adherends while pressure is applied, which may not be possible when manufacturing large and complex parts. In wind turbine blades, for example, adhesive bondlines of up to 30 mm may be required due to large manufacturing tolerances [4,11]. In addition, ultrasonic welding may not be suitable for joining thick sections as vibrations are attenuated through the adherend thickness [12,13]. There is therefore uncertainty about the commercial application of polymer welding in the wind power industry, and to the best of our knowledge there has not been a published demonstration of welding applied to wind turbine blades.

An alternative method of joining acrylic composite parts termed ‘resin welding’ is proposed in this paper. Thermoplastics like acrylics can not only melt but can also dissolve in appropriate solvents. This property has been used to join thermoplastics via *solvent welding* and *solvent cementing*, in which the application of a solvent, rather than heat

as in fusion welding, allows for polymer chain mobility and subsequent interdiffusion and bonding of the thermoplastic polymer. However, residual solvent remains in the polymer and weakens the joint [14,15]. Interestingly, methyl methacrylate monomer is also a solvent for acrylic polymer and is available in commercial formulations to solvent weld PMMA [16]. This provides an opportunity to avoid the weakening effects of solvent welding as, if the acrylic monomer is mixed with an initiator as in some commercial formulations [17], the monomer will act as a reactive solvent and polymerise around the existing polymer network, forming a semi-interpenetrating polymer network (semi-IPN) rather than remaining as a monomer and weakening the joint. A comparison of the different methods is provided in Fig. 1.

In this work, the concept of solvent welding is extended to the joining of acrylic-matrix composite parts by the vacuum infusion of acrylic monomer resin (Elium®) into a joint packed with reinforcement fibre, followed by room temperature polymerisation, allowing for joining with large and varying bondlines with no requirement for heat input. The resin is believed to partially dissolve the matrix at the joining interface and form a semi-IPN after polymerisation, as described previously, creating a continuous, homogeneous material across the joint. This joining method has been termed ‘resin welding’.

In the following sections, the resin welding method is introduced, and the strengths of resin-welded single lap shear specimens are reported and compared with adhesively bonded coupons and welded coupons from the literature. The effect of including filler glass fibres between the adherends with 0° and 90° orientations is explored, as is the effect of changing the bondline thickness from 0.5 mm to 1 mm. The bonding mechanisms are then investigated, firstly through fractographic analysis of the single lap shear coupons’ fracture surfaces, and then by examining the interface between dyed acrylic resin and clear cast acrylic polymer for signs of dissolution of the polymer and formation of a semi-IPN.

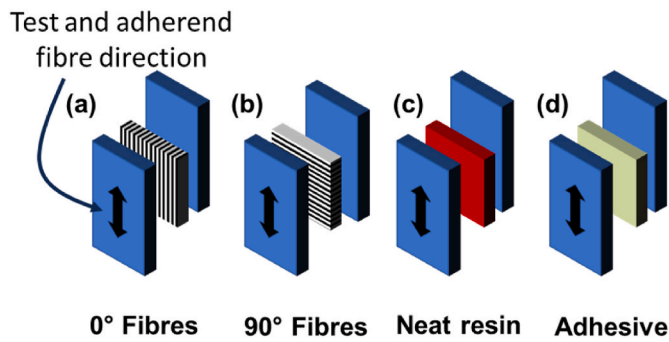


Fig. 2. The four types of single lap joint which were manufactured. Specimens were made with: (a) 0° fibres in the bondline, oriented in the same direction as testing and the fibre direction of the adherends; (b) 90° fibres which were placed perpendicular to the test direction; (c) neat acrylic resin with no fibres in the joint; and (d) an adhesive rather than acrylic resin.

2. Materials and methods

2.1. Single lap coupon manufacturing and testing

2.1.1. Laminate preparation

Glass fibre reinforced acrylic (GF/acrylic) laminates were prepared using a $[0^{\circ}_4]$ layup of 646 g/m² unidirectional non-crimp E-glass fibre fabric (TEST2594-125-50, Ahlstrom-Munksjö) with multi-compatible sizing for a total thickness of 2 mm. Laminates were prepared through the vacuum infusion of Elium® 188 O acrylic monomer resin (Arkema) mixed in a 100:3 wt ratio with BP-50-FT peroxide initiator (United Initiators). The resin polymerised at room temperature for 24 h before cutting with a water-cooled diamond-tipped saw.

2.1.2. Bonding methodology

Single lap shear coupons are commonly used to characterise adhesive strengths, and previous work published on welding acrylic-matrix composites uses single lap shear geometry [5,7,10]. The single lap geometry specified by ASTM D5868 was therefore chosen to allow for comparisons with published values. This was achieved by bonding two GF/acrylic adherend laminates with a 25 mm overlap from which 5 single lap coupons of 25 mm width (and therefore 25 × 25 mm joint area) were cut. The coupons were prepared so that the adherend

reinforcement was parallel to the test direction.

Four types of bonds were prepared: resin-welded joints with neat resin, 0° fibres or 90° fibres in the bondline, and adhesive joints (Fig. 2). Two bond line thicknesses (0.5 mm and 1 mm) were manufactured for each bond type to match the thickness of 1 and 2 plies of GF fabric.

Adhesively joined specimens were prepared using Plexus MA310 two-part methacrylate adhesive, which has been previously shown to have good compatibility with acrylic-matrix composites [5]. The adhesive was applied between the adherends using a mixer nozzle and the bondline thickness was set using wire spacers of either 0.5 mm or 1 mm diameter. Pressure was applied using binder clips and the adhesive was left to cure at room temperature.

Resin-welded joints with reinforcement in the weld were prepared by placing glass fabric in the bondline between two adherend laminates (Figs. 2 and 3). Vacuum bagging, a resin inlet and a vacuum outlet were then attached using an epoxy adhesive to seal the weld region. Vacuum was applied and acrylic resin mixed with initiator was infused and left to polymerise for 24 h to allow the adherends to bond. Joints with neat resin in the bondline were prepared in a similar manner but using wire spacers instead of fabric to set the thickness.

The vacuum bagging, epoxy adhesive and tubing were then removed, and single lap coupons were cut with a diamond-tipped water-cooled saw (Fig. 4a). Composite tabs were applied to reduce loading eccentricities during testing (Fig. 4b). Five coupons were cut for each weld type and thickness, and the 90° and neat resin welds at 1 mm thickness were repeated to give a total of ten coupons for each. Out of the samples cut, only 3 samples each were successfully tested from the 0° fibre welds.

2.1.3. Mechanical testing

Single lap shear coupons were tested in tension according to ASTM D5868 using an Instron 3369 test machine with a 50 kN load cell. A crosshead extension rate of 1 mm/min was selected due to the lower ductility of acrylic resin compared to typical adhesives. The sides of the coupons were speckled with spray paint so that deformations could be tracked using the GOM Correlate Digital Image Correlation (DIC) software.

2.1.4. Statistical analysis

Statistical analysis of the weld strengths was performed using Mini-tab® 20 statistical software. A Welch's ANOVA test ($\alpha = 0.05$) was employed, followed by a Games-Howell post-hoc test.

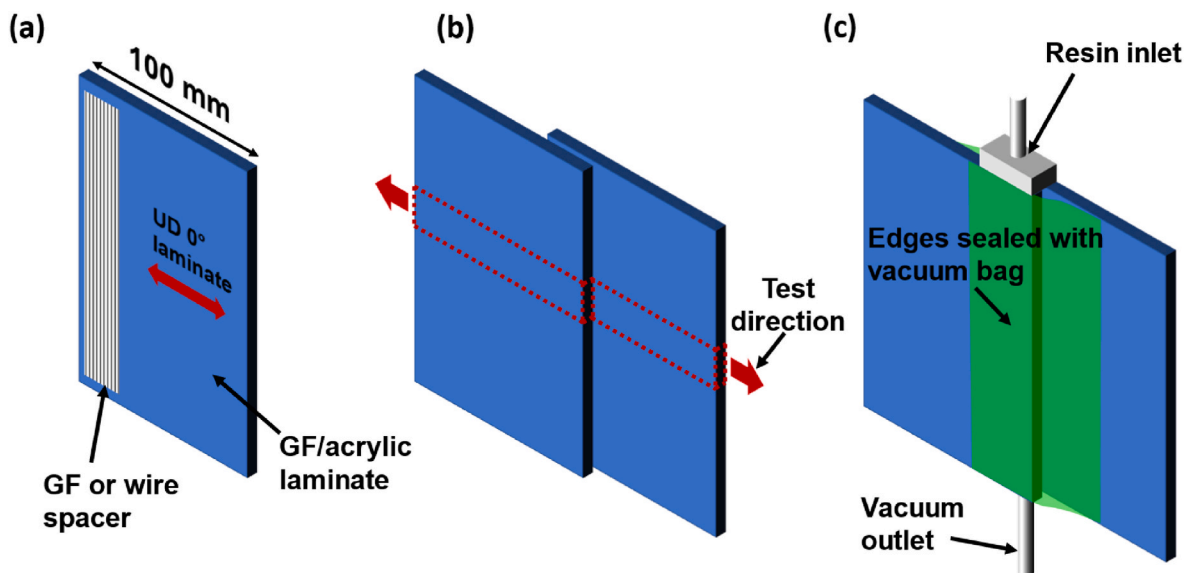


Fig. 3. Details of the resin-welding process. (a) Glass reinforcement, or a wire spacer for adhesive and neat-resin bonds, is placed on the adherend then (b) a second adherend is placed on top—the coupon outline and test direction are highlighted—and (c) the weld region is sealed with vacuum bagging and a resin inlet and outlet.

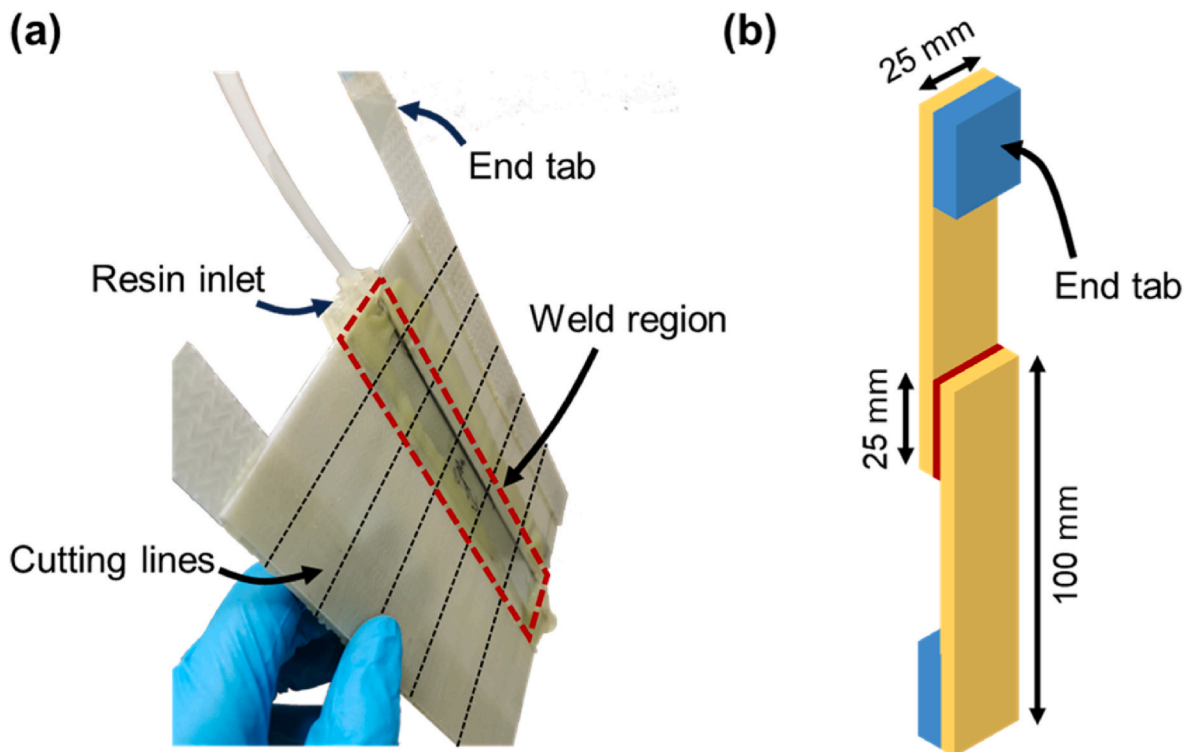


Fig. 4. (a) A prepared weld with lines depicting where coupons are cut in black, and the weld region highlighted in red. (b) The single lap coupon geometry with tabs applied. (For interpretation of the references to colour in this figure legend, the reader is referred to the Web version of this article.)

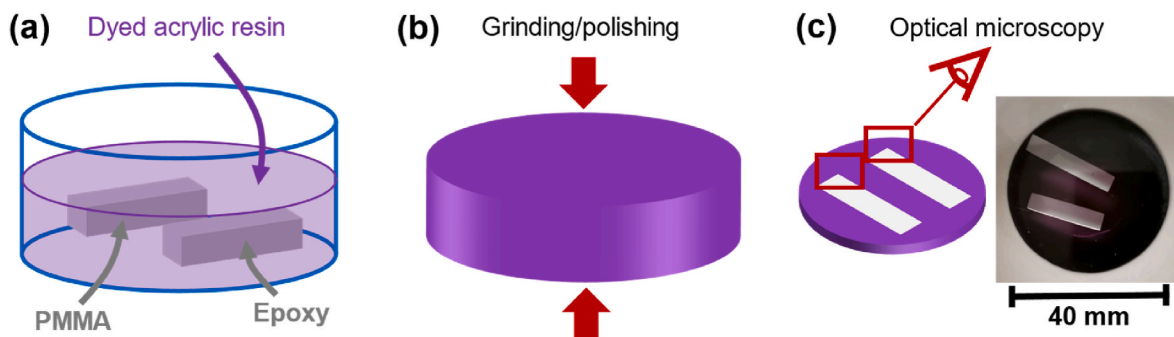


Fig. 5. Specimens were prepared for optical microscopy by (a) immersing PMMA and epoxy coupons in dyed acrylic resin then (b) grinding and polishing the demoulded cylinder. The finished coupon is depicted in (c), and the observed regions are highlighted.

2.1.5. Fractography

Scanning electron microscopy (SEM) was used to observe the fracture surfaces of the single lap shear coupons after testing. The fracture surfaces were sputter-coated with 30 nm of gold and were imaged at 15 kV using a JEOL JSM series electron microscope.

2.2. Investigation of the proposed bonding mechanism

The bonding mechanism that occurs during resin welding was investigated by comparing the diffusion of acrylic resin in PMMA and epoxy polymers using optical microscopy. Epoxy was included for comparison since thermosets do not dissolve in solvents and should therefore not bond via extensive semi-IPN formation, resulting in a difference between the acrylic-acrylic and acrylic-epoxy interfaces.

Cuboids of clear cast PMMA and epoxy were cut and placed into a sample cup of 40 mm diameter which was coated in release agent. Elium® 188 O acrylic resin was dyed with Bestoil Blue 2 N (FastColours Ltd.)—a solvent/oil soluble dye—then mixed in a 100:3 ratio with BP-

50-FT peroxide initiator. The resin was then poured into the sample cup to immerse the polymer cuboids (Fig. 5a). The dye allowed diffusion of the resin to be observed visually, and Bestoil Blue 2 N was chosen for its resistance to bleaching during the free-radical polymerisation of the acrylic. The resin was left to polymerise for 24 h, and the resulting cylinder was demoulded then ground and polished (Fig. 5b) to a thin disc to reveal the immersed polymers for optical microscopy (Fig. 5c).

Grinding and polishing were performed using a water-cooled ATA Saphir 520 polisher. The coupon was first ground to the correct thickness using a P180 grinding disc, and was then polished using a force of 30 N with increasingly fine polishing discs (P400, P800, P1200, P2500, 3 μm and 1 μm) for approximately 3 minutes on each side.

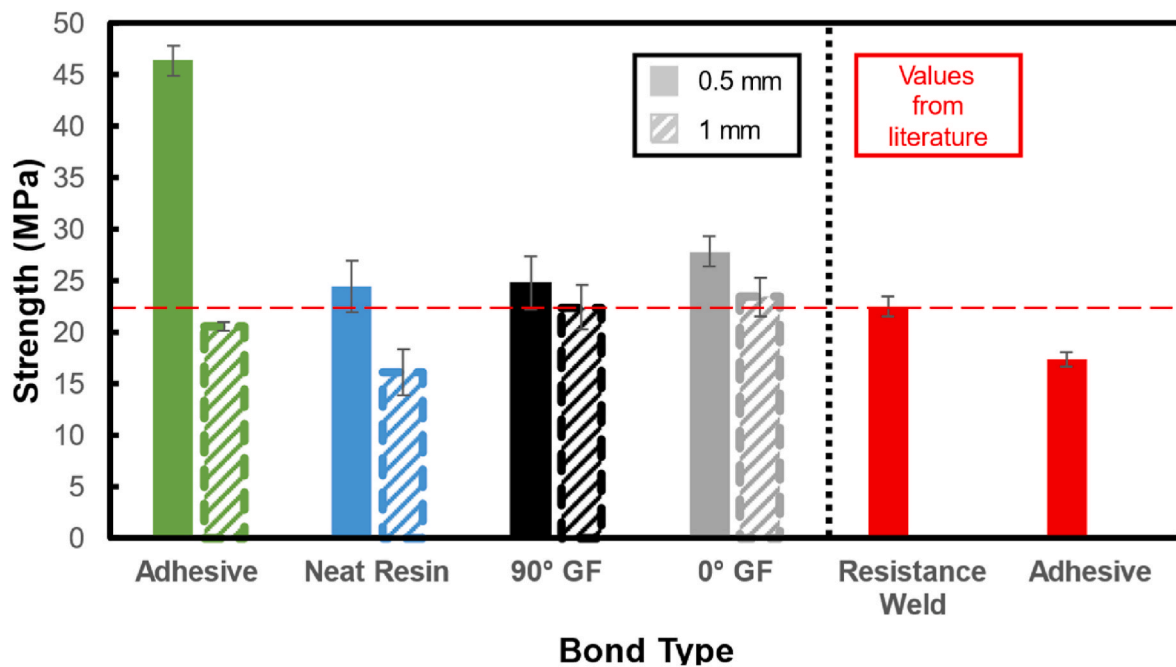


Fig. 6. The single lap shear strengths of each joint type. The values for 0.5 mm thick bonds are solidly coloured and the values for 1 mm thick bonds are hatched. Error bars represent ± 1 standard deviation. A comparison with the highest published weld and adhesive strengths for acrylic-matrix composites [5] is included in red on the right. (For interpretation of the references to colour in this figure legend, the reader is referred to the Web version of this article.)

3. Results and discussion

3.1. Single lap shear testing

3.1.1. Mechanical properties

The single lap shear strengths for each joint type and thickness are shown in Fig. 6. The bond strength of the resin-welding method is promising overall as the highest average weld strength obtained—0.5 mm of 0° fibre reinforcement—reached 27.9 MPa. This is 24 % higher than the strongest reported single lap weld of acrylic-matrix composites in the literature: resistance-welded GF/acrylic adherends ([0°₄] layup of 1200 g/m² fabric, 3.5 mm thickness) with a biaxial carbon fibre heating element [5].

The effect of including fibres in the bondline can be found by comparing the strengths of the bonds with fibres to the bonds with neat resin. Considering first the 0.5 mm bondlines, the welds with 0° fibres, 90° fibres and neat resin had strengths which were not significantly different according to the statistical analysis. The highest strength of 46.4 MPa was obtained with adhesive and a bondline of 0.5 mm, 66.4 % greater than the 0.5 mm weld with 0° fibres ($P = 0.000$).

This study therefore measures no significant effect of fibre type, or if there is an effect it is too small in magnitude to observe under the parameters of the study. Other studies have measured a much greater effect on single lap shear strength of including unidirectional reinforcement in adhesive bondlines. Khalili et al. tested the single lap shear strength of GF/polyester adherends bonded with epoxy adhesive reinforced with unidirectional 0° glass fibres, resulting in a 54 % increase in strength (18.4 MPa vs. 11.9 MPa) over neat adhesive bonds [18]. Delzendehrooy et al. similarly compared the single lap shear strength of aluminium adherends bonded with epoxy adhesive and date palm fibre reinforced epoxy adhesive. Bonds reinforced with 0° fibres reached a strength up to 98 % greater than those with unreinforced adhesive [19]. Finally, Behera et al. tested both aluminium-to-composite (GF/epoxy) and aluminium-to-aluminium bonds with 0° glass fibre reinforced adhesive [20]. In comparison with neat adhesive, the reinforced adhesive increased single lap shear strength by 27.3 % in aluminium-to-aluminium bonds and by 45.4 % in

aluminium-to-composite bonds.

The effect of heating element fibre orientation in the welding of thermoplastic composites has also been studied in the literature, although comparisons between fibre orientations may be complicated by the changes in welded area and thermal uniformity that different heating element fabrics create in resistance and induction welding [5, 21]. In one study by Tanabe et al. [21], CF/PPS composites were joined using resistance welding, with carbon fibre heating elements in either the 0° or 90° direction. Similar welded areas were achieved using each fibre direction but changing the heating element fibre orientation from 90° to 0° increased the single lap shear strength by 65 %, from 16.5 MPa to 27.2 MPa.

The key difference between these studies and the present work is the fracture behaviour of the coupons. In each of these studies there was at least partial cohesive failure, and fracture occurred through the adhesive reinforcement or heating element fibres. The fibres therefore contributed to the single lap shear strength by resisting crack propagation. However, as will be discussed further in Section 4.1.2, crack propagation in the present study initiated via peeling at the edges and continued through the upper layer of the adherends for all coupons, rather than through the bondline. Therefore, the reinforcement in the bondline was unable to contribute significantly to an increase in strength.

The effect of increasing thickness differs depending on the bond type. Although the Plexus MA310 adhesive had a high single lap shear strength (46.4 MPa) with a 0.5 mm bondline the adhesive bond strength saw a large drop of 56 % ($P = 0.000$) as thickness increased to 1 mm. The neat-resin bonds also saw a large drop in strength of 34 % ($P = 0.005$) from 24.5 MPa to 16.2 MPa as the thickness was increased. Decreases in single lap shear strength with increasing bondline thickness have also been reported in the literature and have been attributed to greater peel and shear stresses and an increased likelihood of voids and other imperfections [22–24]. In contrast, the mean strength of bonds with 90° fibres and 0° fibres decreased by only 11 % and 16 % respectively with increasing thickness, which were therefore not found to be statistically significant changes ($P = 0.584$ and $P = 0.238$ respectively). The inclusion of fibres in the bond therefore appears to have benefits in thicker bondlines.

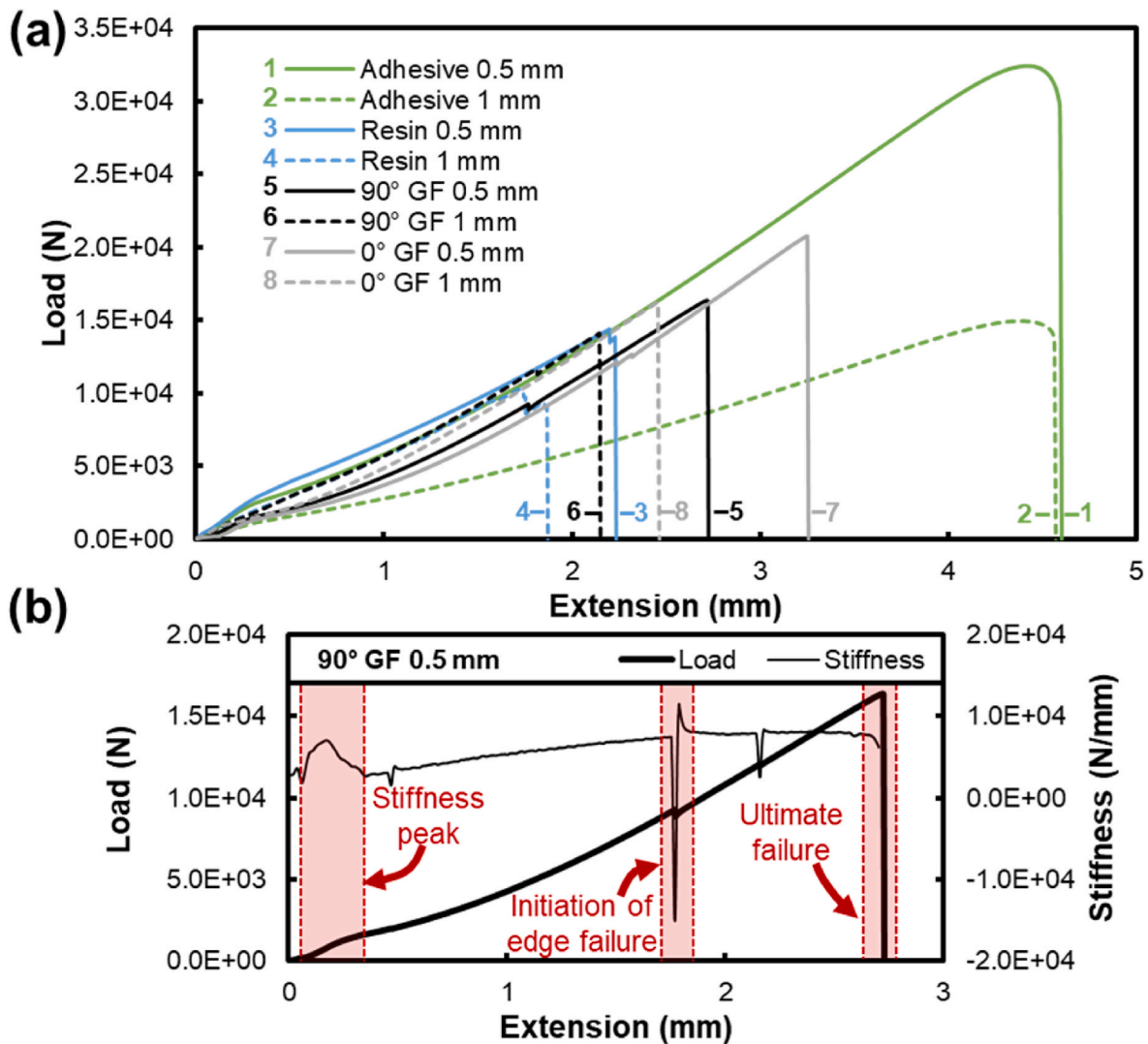


Fig. 7. (a) Representative load-extension curves for each type of single lap bond. Bonds of the same type are the same colour, with the 0.5 mm bond having a solid line and the 1 mm bond having a dashed line. (b) The representative load-extension curve of the 90° GF 0.5 mm coupon along with its derivative i.e. the variation in stiffness of the coupon throughout the test. The initial peak in stiffness, the initial edge failure—which is also visible as a small drop in the load-extension curve—and the ultimate failure are highlighted in red for both the load and stiffness curves. (For interpretation of the references to colour in this figure legend, the reader is referred to the Web version of this article.)

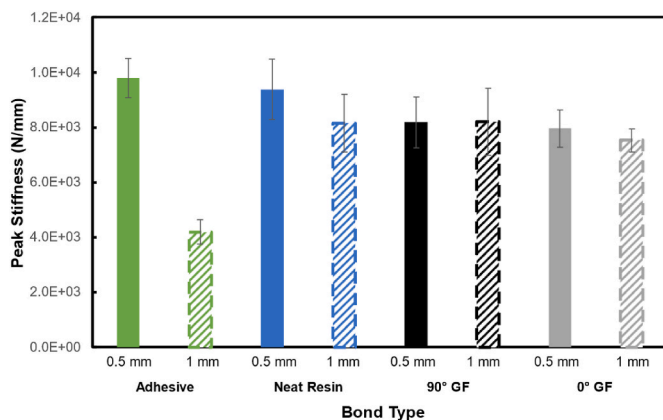


Fig. 8. The average peak gradient of the load-extension curves for each bond type below 0.5 mm extension. The 1 mm adhesive bond has a significantly lower stiffness than the rest.

These results show that increasing bondline thickness has a significant detrimental effect on adhesive bond strength; indeed, Plexus MA310 has a maximum recommended thickness of just 3.2 mm according to its technical datasheet [25] and would therefore be unsuitable for use in the thick bondlines found in wind turbine blades. Other adhesives which are designed for use in thick bondlines are available, but their strengths are significantly lower [5,26], and failure in adhesives is therefore common in wind turbine blades due to the relative weakness of these thick adhesive bonds, and the likelihood of them containing defects [27]. The presented results therefore suggest that resin welding could serve as a viable alternative to adhesives in wind turbine blades and other large structures. In resin welding, the bondlines are not constrained to the same maximum thickness as adhesives and could reach the same thickness as the thick-section composites being joined.

This effect of bondline thickness would partly explain discrepancies with the published single lap shear strength of 17.4 MPa for GF/acrylic coupons joined by MA310 adhesive published by Murray et al. [5], which was conducted with a bondline thickness of 0.76 mm. For comparison, the adhesive’s technical datasheet suggests a single lap shear

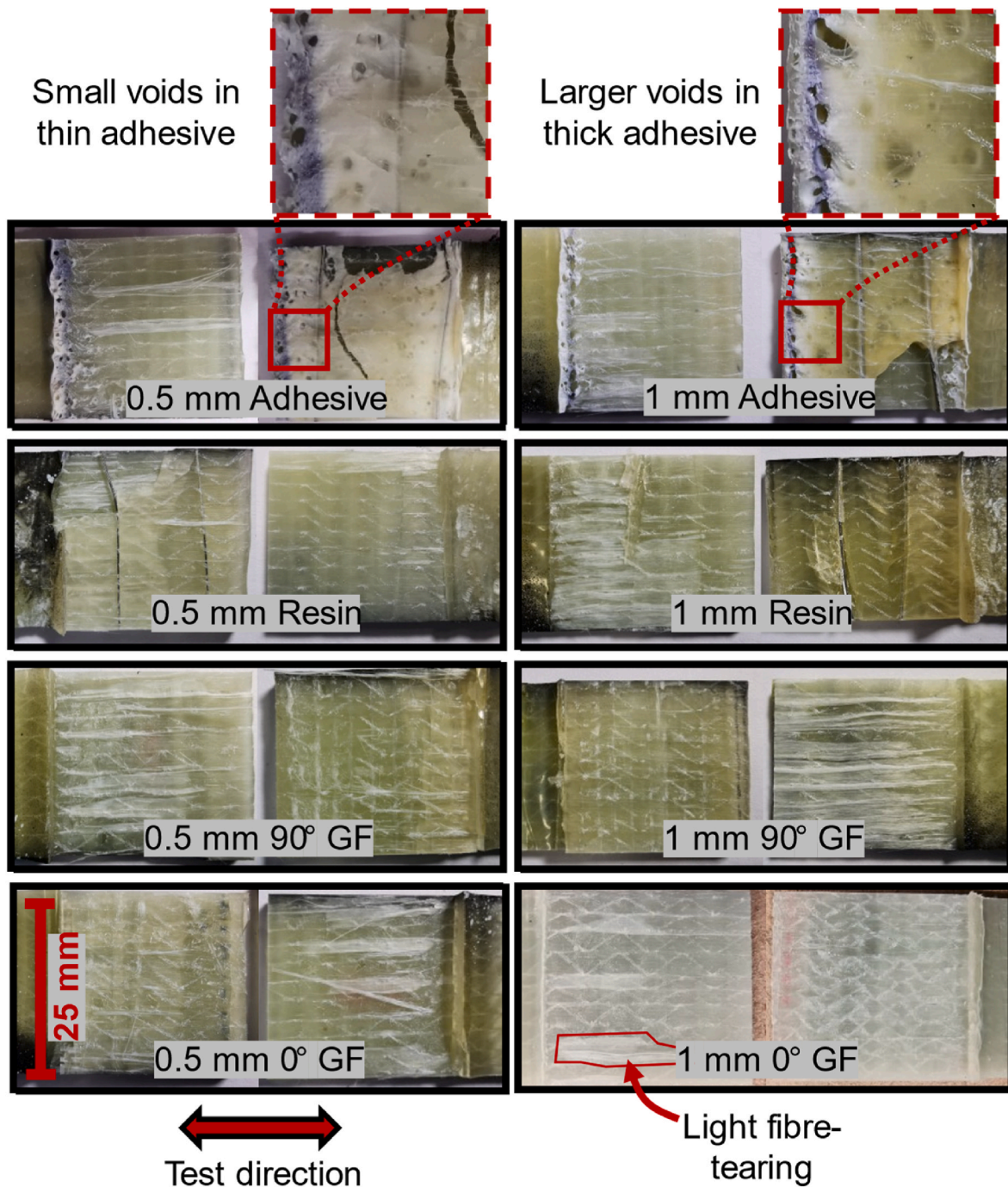


Fig. 9. Representative fracture surfaces of the tested single lap coupons. Each image is of both halves of a fractured coupon. The crack propagation direction (the testing direction) is shown. Light fibre tearing is highlighted in the 1 mm 0 GF coupon, but it is visible in all fracture surfaces. The voids present in both adhesive bonds are shown at higher magnification, and larger voids are visible in the 1 mm thick adhesive. Voids were not visible in the resin welded coupons.

strength range of 20.7–24.1 MPa [25]. The edge quality of the specimens could also play a role as Murray et al. allowed the adhesive to spill out the edges, whereas in the present study the edges were shaped to match the edges of the resin-welded specimens more closely, possibly reducing stress concentrations and increasing strength [28].

Representative load-extension curves for each bond type are provided in Fig. 7. A ductile failure of the adhesive bonds is evident compared to the brittle fractures of the weld specimens. It should also be noted that the 0.5 mm and 1 mm adhesive bonds reached similar average extensions before failure (4.6 ± 0.1 mm and 4.3 ± 0.2 mm respectively) despite the latter's significantly lower strength. The stiffness of the 1 mm adhesive bond is therefore lower than that of the 0.5

mm adhesive bond, however comparisons between the bond stiffnesses is made difficult by the shapes of the load-extension curves.

Although an initial linear load-extension response for composite single lap shear bonds is reported in some publications [29], allowing stiffnesses to be easily calculated, in this case the load-extension curves have an initial s-shape below approximately 0.5 mm extension followed by a gradually increasing gradient. Therefore, in order to compare the stiffnesses of the single lap coupons, the load-extension curves are differentiated. The resulting stiffness vs. extension curves have a shape similar to that in Fig. 7b in which there is an initial peak in stiffness. Loading in single lap joints is complex and is a mixture of shear and peel which is accompanied by the bending of the adherends. The reason for

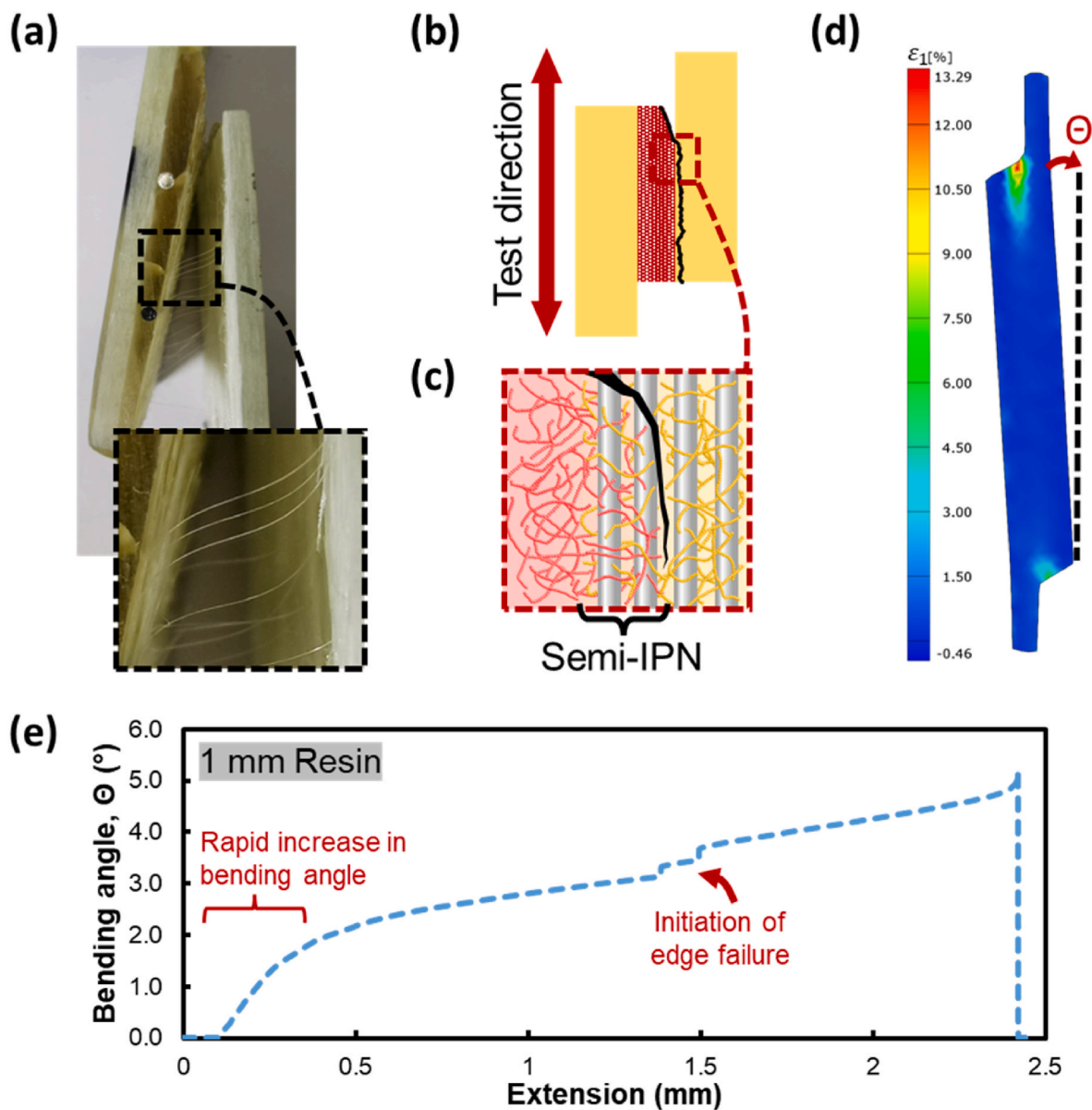


Fig. 10. Fibre bridging in a coupon bonded with neat resin (no reinforcement). The bridging fibres therefore come from the surface of the adherend. (b) The failure mode of the welded coupons was light fibre tearing where a small amount of glass fibre is removed from the adherend surface (c) The fracture propagation was through the adherend matrix (yellow) rather than through the tougher semi-IPN. (d) A representative map of major strain in a single lap coupon close to failure. Stress concentrations are found at the edges of the overlap region. The rotation of the specimens during testing (θ) is highlighted. (e) A representative bending angle vs. extension curve for a 1 mm resin weld. The rapid increase in bending angle corresponding to the stiffness peak is highlighted. (For interpretation of the references to colour in this figure legend, the reader is referred to the Web version of this article.)

the nonlinear curve shape was therefore investigated by measuring the bending angle of the coupons using DIC (Fig. 10e). Below 0.5 mm extension, there is a rapid increase then subsequent slowing in bending rate, therefore the initial peak in stiffness (Fig. 7b) can be attributed to the bending of the adherends. The average peak in gradient before 0.5 mm extension for each joint is summarised in Fig. 8. Only the 1 mm adhesive joint has a significantly lower peak stiffness of 4.2 kN/mm due to the low modulus and high ductility of the adhesive, which makes a greater contribution to stiffness at higher bondline thicknesses.

3.1.2. Failure modes and mechanisms

Images of the failed coupons are shown in Fig. 9.

The failure modes of the adhesive and resin-welded coupons can be classified as light fibre tear failure (ASTM D5573) as, rather than the more common adhesive or cohesive failure types, a small amount of

resin and glass fibre is removed from the surface of the adherend. The clearest evidence of this is the fibre bridging in coupons with no fibres in the bondline (Fig. 10a), indicating that these fibres must come from the adherend. It is therefore the adherend matrix that fails rather than the bond between the infused resin and the adherend matrix (Fig. 10b and c). This is confirmed via SEM imaging which showed that 0° fibres were present in the fracture surfaces of all coupons, regardless of whether or not 0° fibres were placed in the bondline.

Representative SEM images are presented in Fig. 11 and depict both halves of a coupon bonded with 0.5 mm of neat acrylic resin. The presence of fibres on both sides—despite no fibres being included in the bondline—shows that the crack propagates within the first layer of the adherend fibres (light fibre tearing). These results suggest that the formation of a semi-IPN increases fracture toughness compared to the bulk polymer, leading to failure in the adherend matrix rather than in the

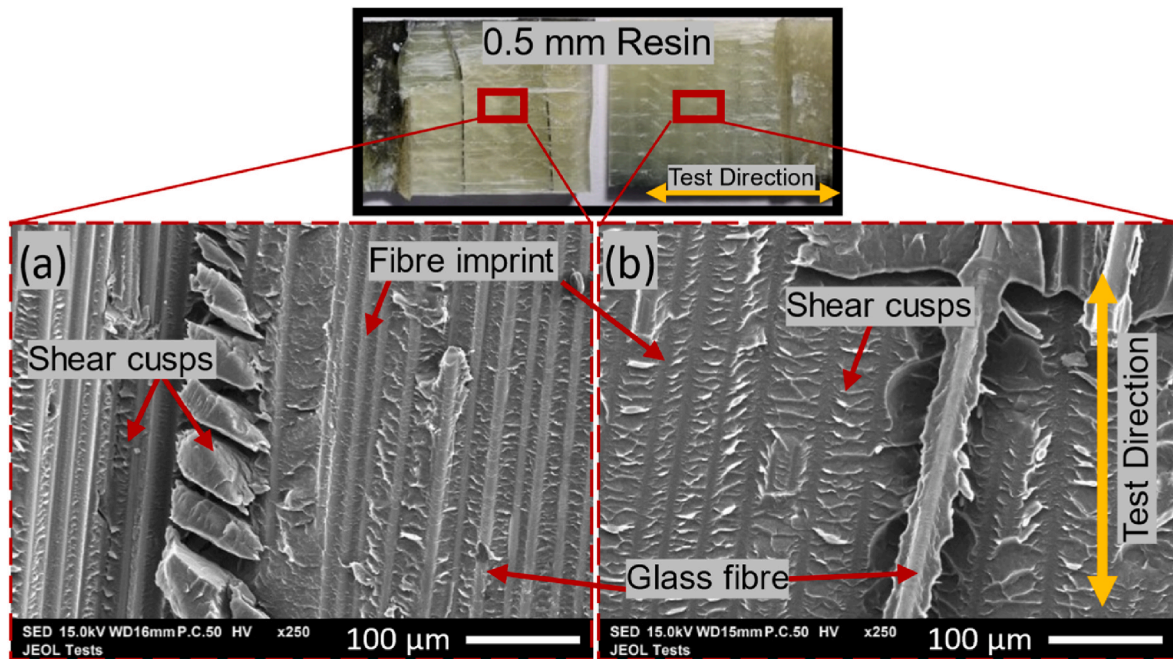


Fig. 11. SEM images of the fracture surfaces of GF/acrylic bonded with 0.5 mm of neat acrylic resin. Photographs of the imaged fracture surfaces are provided above, with the imaged areas represented by red rectangles (not to scale). Image (a) is of one half of a fractured single lap shear coupon and image (b) is of the other half. Fibres and imprints are present in both halves indicating light fibre tearing of the adherend. Cusps indicate a shear failure. (For interpretation of the references to colour in this figure legend, the reader is referred to the Web version of this article.)

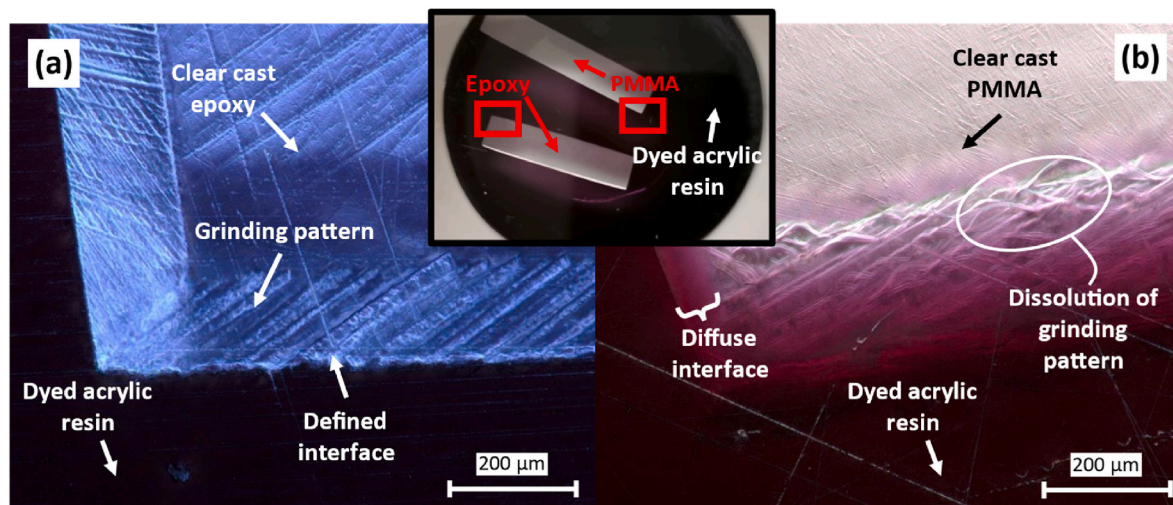


Fig. 12. Optical microscope images of the edges of (a) epoxy and (b) PMMA cuboids immersed in dyed acrylic resin. A lower magnification photograph of the epoxy and PMMA cuboids cast in dyed acrylic resin is shown in the centre of the figure. The optical microscopy imaging locations are highlighted with red rectangles. (For interpretation of the references to colour in this figure legend, the reader is referred to the Web version of this article.)

semi-IPN at the bonding interface, as shown schematically in Fig. 10b and c.

Further insight into the failure of the coupons was gained using DIC. A map of the major strain across the profile of a single lap coupon just before failure is presented in Fig. 10d. As noted in the literature [30], there are stress concentrations at the edges of the overlap region, and this is therefore where failure initiates. The rotation of the specimens during testing means that this is a concentration of both shear and peel forces [28,31], but failure was observed to initiate via peeling at the edges. However, shear cusps are present in the SEM images in Fig. 11a and b, therefore failure proceeds via a mixture of shear and peeling.

3.2. Bonding mechanism

Adhesives can bond via several mechanisms, including the formation of chemical or physical bonds with the adherend surface, mechanical interlocking between the adhesive and a rough adherend surface, via electrostatic attraction or through diffusive bonding [32,33]. Since PMMA is soluble in its monomer, the resin-welding method is expected to create a bond via dissolution, diffusion, and the subsequent formation of a semi-IPN. The experiment described in Section 3.2 allows us to visualise this bond.

Optical microscope images of the interfaces between dyed acrylic resin and clear cast coupons of epoxy and PMMA polymers can be found in Fig. 12a and b respectively. There are two visible differences between

the interfaces of epoxy and PMMA with the acrylic resin. Firstly, there is a difference in colour, as in the epoxy there is a well-defined colour boundary with the dyed resin, whereas in the PMMA there is a colour gradient. The dye molecules therefore diffuse into the PMMA as it is dissolved by the acrylic monomeric resin and remain there once the resin polymerises.

Secondly, there is a difference in morphology at the interface. There are ridges at the edges of the polymer coupons caused by grinding, and in the case of epoxy these are again well-defined and unaffected by the acrylic resin, whereas signs of dissolution are evident in the PMMA specimen (Fig. 12b). This is to be expected as epoxies are thermoset polymers, so they do not dissolve in solvents. This experiment therefore provides evidence for the formation of a semi-IPN as the bonding mechanism, which is only applicable when the polymer is soluble in the infused resin.

The low viscosity of the acrylic resin allows significant penetration of the monomer into the polymer; however, the same bonding mechanism may be expected to occur when bonding GF/acrylic with Plexus MA310 due to its MMA content. The similarity in failure mechanisms between the resin welds and the adhesive bonds—light fibre-tearing (Fig. 10)—would support this, although the high viscosity and short working time of the adhesive (approximately 15 min vs. 90 min for the acrylic resin) may limit semi-IPN formation.

4. Conclusions

Welded bonds in acrylic-matrix composites have been shown in the literature to increase static strength and fatigue life over adhesive bonds, but improvements in manufacturing tolerances must be made if they are to be applied to large structures like wind turbine blades. The technique introduced in this work—*resin welding*—has been shown to be a promising joining alternative for acrylic-matrix composites. As with traditional welding methods, resin welding also results in the entanglement of PMMA chains at the bonding interface. However, in resin welding, instead of heating and melting the polymer chains, acrylic monomer resin is infused into a bondline packed with reinforcement fibres. Here, the resin dissolves and diffuses into the acrylic matrix of the adherends, polymerising around the existing polymer and leading to the formation of a semi-IPN, as evidenced by the diffusion of dyed acrylic resin into clear cast PMMA.

The single lap shear strength of resin welded coupons reached a maximum of 27.9 MPa with a 0.5 mm bondline packed with 0° glass fibres, a strength 24 % higher than the highest published value for welded acrylic-matrix composites [5]. Nevertheless, this strength was exceeded by bonds prepared with a methacrylate adhesive, which reached 46.4 MPa with a 0.5 mm bondline. Unlike the resin welded bonds, however, the adhesive strength and stiffness were highly affected by thickness, and the strength dropped by 56 % and the stiffness by 57 % when thickness was increased to 1 mm.

Methacrylate adhesives may therefore be the most appropriate joining method for acrylic-matrix composites when bondlines are thin as they create strong bonds, but their strength quickly drops with increasing thickness. Welding methods like ultrasonic, resistance or induction welding also result in high bond strengths, but they generally require intimate contact between the adherends. As a result, thicker bondlines like those found in wind turbine blades may benefit from resin welding, and further investigation of the method in large structures is therefore warranted with the continuing development of recyclable acrylic-matrix wind turbine blades.

CRediT authorship contribution statement

Machar Devine: Conceptualization, Data curation, Formal analysis, Investigation, Methodology, Project administration, Resources, Visualization, Writing – original draft, Writing – review & editing. **Ankur Bajpai:** Conceptualization, Data curation, Formal analysis,

Investigation, Methodology, Project administration, Resources, Visualization, Writing – review & editing. **Conchúr M. Ó Brádaigh:** Funding acquisition, Resources, Supervision, Validation, Writing – review & editing. **Dipa Ray:** Conceptualization, Funding acquisition, Methodology, Project administration, Resources, Supervision, Validation, Visualization, Writing – review & editing.

Declaration of competing interest

The authors declare that they have no known competing financial interests or personal relationships that could have appeared to influence the work reported in this paper.

Data availability

Data will be made available on request.

Acknowledgements

The authors are grateful for funding provided by the Wind and Marine Energy Systems and Structures Centre for Doctoral Training (CDT-WAMSS), to the University of Edinburgh EPSRC IAA for funding received through block grant EP/R511687/1, and to the Supergen ORE Hub for funding received through the Flexible Fund Award FF2021-1014. The authors gratefully acknowledge Arkema GRL, France for the provision of materials towards this research.

References

- [1] Obande W, Ó Brádaigh CM, Ray D. Continuous fibre-reinforced thermoplastic acrylic-matrix composites prepared by liquid resin infusion – a review. *Compos B Eng* 2021;215.
- [2] Obande W, Mamalis D, Ray D, Yang L, Ó Brádaigh CM. Mechanical and thermomechanical characterisation of vacuum-infused thermoplastic- and thermoset-based composites. *Mater Des* 2019;175.
- [3] Denis Y, Siddig N, Guitton R, Le Bot P, De Fongalland A, Lecoite D. Thermochemical modeling and simulation of glass/elium® acrylic thermoplastic resin composites. *Materials Research Proceedings* 2023;28:313–20.
- [4] Subrahmanian KP, Dubouloz F. Adhesives for bonding wind turbine blades. *Reinforc Plast* 2009;53(1):26–9.
- [5] Murray RE, Roadman J, Beach R. Fusion joining of thermoplastic composite wind turbine blades: lap-shear bond characterization. *Renew Energy* 2019;140:501–12.
- [6] Ageorges C, Ye L, Hou M. Advances in fusion bonding techniques for joining thermoplastic matrix composites: a review. *Compos Appl Sci Manuf* 2001;32(6): 839–57.
- [7] Bhudolia SK, Gohel G, Fai LK, Barsotti RJ. Investigation on ultrasonic welding attributes of novel carbon/Elium® composites. *Materials* 2020;13(5):10–5.
- [8] Bhudolia SK, Gohel G, Kantipudi J, Leong KF, Barsotti RJ. Ultrasonic welding of novel carbon/elium(R) thermoplastic composites with Flat and integrated Energy directors: lap shear characterisation and fractographic investigation. *Materials* 2020;13(7).
- [9] Bhudolia SK, Gohel G, Kah Fai L, Barsotti RJ. Fatigue response of ultrasonically welded carbon/Elium® thermoplastic composites. *Mater Lett* 2020;264:127362.
- [10] Perrin H, Bodaghi M, Berthe V, Vaudemont R. On the addition of multifunctional methacrylate monomers to an acrylic-based infusible resin for the weldability of acrylic-based glass fibre composites. *Polymers* 2023;15(5).
- [11] Zarouchas D, Nijssen R. Mechanical behaviour of thick structural adhesives in wind turbine blades under multi-axial loading. *J Adhes Sci Technol* 2016;30(13): 1413–29.
- [12] Bhudolia SK, Gohel G, Leong KF. Advances in ultrasonic welding of thermoplastic composites : a review. 2020.
- [13] Benatar A, Cheng Z. Ultrasonic welding of thermoplastics in the far-field. *Polym Eng Sci* 1989;29(23):1699–704.
- [14] Chapter 16 - solvent welding. In: Troughton MJ, editor. *Handbook of plastics joining*. second ed. Boston: William Andrew Publishing; 2009. p. 139–43.
- [15] Lin CB, Lee S, Liu KS. The microstructure of solvent-welding of PMMA. *J Adhes* 1991;34(1–4):221–40.
- [16] RS Pro. *Anglosol 12: SDS No. CP1205 v1.11 RS 144-406 2022* [Online]. Available: <https://docs.rs-online.com/3a29/0900766b80980339.pdf>.
- [17] RS Pro. *Anglosol 70 Part A: SDS No. CP1187A v1.12 RS 144-399 2022* [Online]. Available: <https://docs.rs-online.com/2e2b/0900766b809599ae.pdf>.
- [18] Khalili SMR, Shokuhfar A, Hoseini SD, Bidkhorji M, Khalili S, Mittal RK. Experimental study of the influence of adhesive reinforcement in lap joints for composite structures subjected to mechanical loads. *Int J Adhesion Adhes* 2008;28 (8):436–44.

- [19] Delzendehrooy F, Ayatollahi MR, Akhavan-Safar A, da Silva LFM. Strength improvement of adhesively bonded single lap joints with date palm fibers: effect of type, size, treatment method and density of fibers. *Compos B Eng* 2020:188.
- [20] Behera RK, Parida SK, Das RR. Effect of using fibre reinforced epoxy adhesive on the strength of the adhesively bonded Single Lap Joints. *Compos B Eng* 2023:248.
- [21] Tanabe D, Nishiyabu K, Kurashiki T. Electro fusion joining of carbon fiber reinforced thermoplastic composites using carbon fiber heating element. In: 16th European conference on composite materials, ECCM 2014; 2014.
- [22] Gleich DM, Van Tooren MJL, Beukers A. Analysis and evaluation of bondline thickness effects on failure load in adhesively bonded structures. *J Adhes Sci Technol* 2001;15(9):1091–101.
- [23] da Silva LFM, Rodrigues TNSS, Figueiredo MAV, de Moura MFSE, Chousal JAG. Effect of adhesive type and thickness on the lap shear strength. *J Adhes* 2006;82(11):1091–115.
- [24] da Silva LFM. Design rules and methods to improve joint strength. In: da Silva LFM, Öchsner A, Adams RD, editors. *Handbook of adhesion technology*. Berlin, Heidelberg: Springer Berlin Heidelberg; 2011. p. 689–723.
- [25] ITW Performance Polymers. *Technical Data Sheet Plexus MA310 Rev 09 2018* [Online]. Available: https://itwperformancepolymers.com/wp-content/uploads/umb/10754/ma310-data-sheet_rev09.pdf.
- [26] ITW Performance Polymers. *Plexus Adhesive Selector Guide EMEA 2023* [Online]. Available: <https://itwperformancepolymers.com/wp-content/uploads/Plexus-Selector-Chart-EMEA.pdf>.
- [27] Mishnaevsky Jr L. Root causes and mechanisms of failure of wind turbine blades: overview. *Materials* 2022;15(9).
- [28] Redmann A, Damodaran V, Tischer F, Prabhakar P, Osswald TA. Evaluation of single-lap and block shear test methods in adhesively bonded composite joints. *Journal of Composites Science* 2021;5(1):27.
- [29] Srinivasan DV, Ravichandran V, Idapalapati S. Failure analysis of GFRP single lap joints tailored with a combination of tough epoxy and hyperelastic adhesives. *Compos B Eng* 2020:200.
- [30] Noble T, Davidson J, Floreani C, Bajpai A, Moses W, Doohar T, et al. Powder epoxy for one-shot cure, out-of-autoclave applications: lap shear strength and Z-pinning study. *Journal of Composites Science* 2021;5:225.
- [31] da Silva LFM, Adams R D. Techniques to reduce the peel stresses in adhesive joints with composites. *Int J Adhesion Adhes* 2007;27(3):227–35.
- [32] Chapter 17 - adhesive bonding. In: Troughton MJ, editor. *Handbook of plastics joining*. second ed. Boston: William Andrew Publishing; 2009. p. 145–73.
- [33] Gardner DJ. Wood: surface properties and adhesion. In: Buschow KHJ, Cahn RW, Flemings MC, Ilschner B, Kramer EJ, Mahajan S, et al., editors. *Encyclopedia of materials: science and technology*. Oxford: Elsevier; 2001. p. 9745–8.